Manipulation and patterning of the surface hydrogen concentration on Pd(111) by electric fields

T. Mitsui, E. Fomin, D.F. Ogletree and M. Salmeron

Lawrence Berkeley National Laboratory. Berkeley, CA 94720. USA

A. U. Nilekar and M. Mavrikakis

Department of Chemical & Biological Engineering

University of Wisconsin-Madison, Madison, WI 53706. USA

[**] Work at LBL was supported by the Director, Office of Energy Research, Office of Basic Energy Sciences, Materials Sciences Division of the U.S. Department of Energy under contract No. DE-AC02-05CH11231. Work at UW was supported by DOE-BES, Division of Chemical Sciences, under contract No. DE-FG02-05ER15731. AUN and MM thank SC Johnson & Son, Inc. for a Distinguished Fellowship. Computational resources at DOE-NERSC, PNNL, and ORNL are gratefully acknowledged.

Modification of the structure of materials at the nanoscale level is one goal of current nanoscience research. For example, by purposefully modifying the spatial distribution of adsorbates one could control the rate of chemical reactions on a local scale. Here we show how this can be accomplished in the case of H on Pd(111) through the application of local electric fields. Hydrogen adsorption on the platinum group metals is particularly interesting because these metals are used as catalysts in a variety of industrial processes, including hydrogenation and dehydrogenation reactions.[1, 2]. Electric fields on surfaces are also of primary interest in electrochemistry[3, 4] where despite the considerable amount of experimental and theoretical work done to date[5-12], there still remains more work to be done before a clear understanding of phenomena at the atomic scale can be accomplished.

In a recent paper, Sykes et al.[13] describe the manipulation of H atoms on Pd(111) using the tip of a scanning tunneling microscope (STM). The authors propose that inelastic excitation by tunneling electrons drives H atoms from the bulk to the subsurface layers. Electronic excitations have also been shown to promote the selective desorption of H atoms from silicon.[14] Using a field ion microscope Kellogg et al. found that strong electric fields enhance the diffusion of metal atoms towards the step edges that decorate the sharp tip.[15] Here we manipulate the concentration of surface H by means of electric fields which, as we will show using Density Functional Theory (DFT) calculations, change the adsorption energy of surface and subsurface H atoms. This drives H away from high-field regions of the surface, as well as into subsurface layers.

The experiments were performed with a variable temperature STM in ultra high vacuum (UHV). The sample temperature could be varied from ca. 40 K to room temperature[16]. The Pd(111) crystal was cleaned by Ar ion sputtering followed by annealing, then exposed to 10 L of hydrogen gas at 60-70K, which produced a coverage between 0.75 and 1 monolayer (ML), as described previously[17, 18]. Upon adsorption, H_2 molecules dissociate readily and the H atoms occupy 3-fold fcc sites, forming three ordered structures as a function of coverage: $\sqrt{3}\times\sqrt{3}$ R30-1H up to 0.33 ML, $\sqrt{3}\times\sqrt{3}$ R30-2H between 0.33 ML and 0.66 ML, and 1x1 between 0.66 ML and 1 ML. In practice, it is difficult to reach coverage of 1 ML because of a significant reduction in the H_2 sticking coefficient with increasing coverage. Indeed, the STM images always show

the presence of numerous residual vacancies. This reflects the fact that H_2 dissociation occurs preferentially at Pd atoms with no adjacent H atoms. These sites are only found when 3 or more vacancies coalesce[19].

Under typical imaging conditions of 50-200 mV bias and 1-15 nA current, H atoms are imaged as ~5 pm depressions, while H-vacancies give rise to ~50 pm protrusions. With the same tunneling parameters the average tip height during imaging is lowest (closer to the surface) for the 1x1 structure, higher for the $\sqrt{3}\times\sqrt{3}$-2H, higher yet for the $\sqrt{3}\times\sqrt{3}$-1H, and highest for the clean surface. Since a linear grey scale is used to represent heights in the figures, it is easy to identify regions of low (high) H concentration in large images by their bright (dark) appearance.

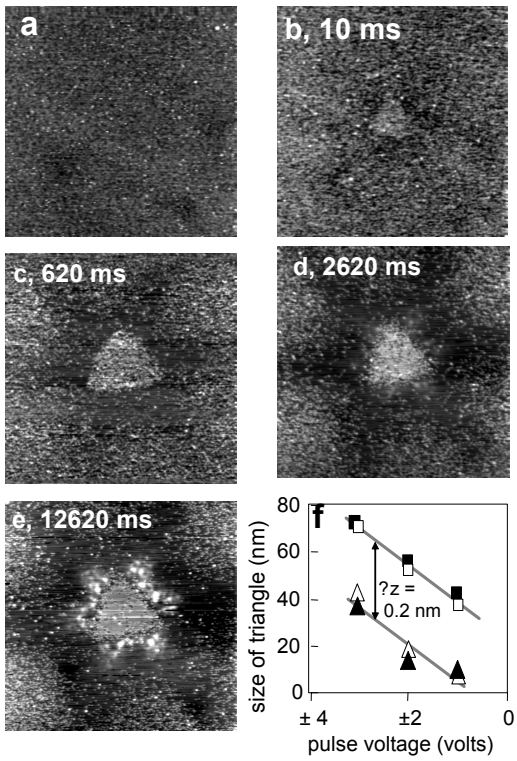

Figure 1. 100x100 nm STM images of Pd(111) at 60K (2nA, 200mV, tip-sample distance ~0.5-0.7 nm) after an exposure to H_2 that produced a coverage close to 1 monolayer. (a) Before application of a voltage pulse near the center. (b) After a 10 ms 2 volt pulse with the tip at the center. (c) Same after an additional 610 ms pulse. (d) After an additional 2000 ms pulse. (e) After an additional 10 s pulse. Bright (dark) regions correspond to low (high) H-coverage. The high electric field near the tip apex during the pulse drives H out of the central region producing a roughly triangular region depleted of H (brighter in the images). (f) Lateral size of the H-depleted triangular region created by a 10 s pulse as a function of voltage. The bottom graph was obtained with the tip approximately 0.2 nm closer to the surface.

The manipulation experiments were performed on a nearly H-saturated surface at temperatures between 40K and 90 K. In figure 1a the tip was positioned near the image center, feedback control was disabled, and the bias voltage increased from its imaging value of 70 mV to the manipulation value of 2 V for 10 milliseconds. After restoring the imaging parameters (15 nA, 70 mV) a new image was acquired, shown in figure 1b. As can be seen, the effect of the voltage pulse was the formation of a roughly triangular patch with higher contrast (bright), due to reduced H coverage, centered at the projected position of the tip during the pulse. The triangular patch is surrounded by a dark region with 6-fold symmetry. Repeating the same experiment for increasingly long times

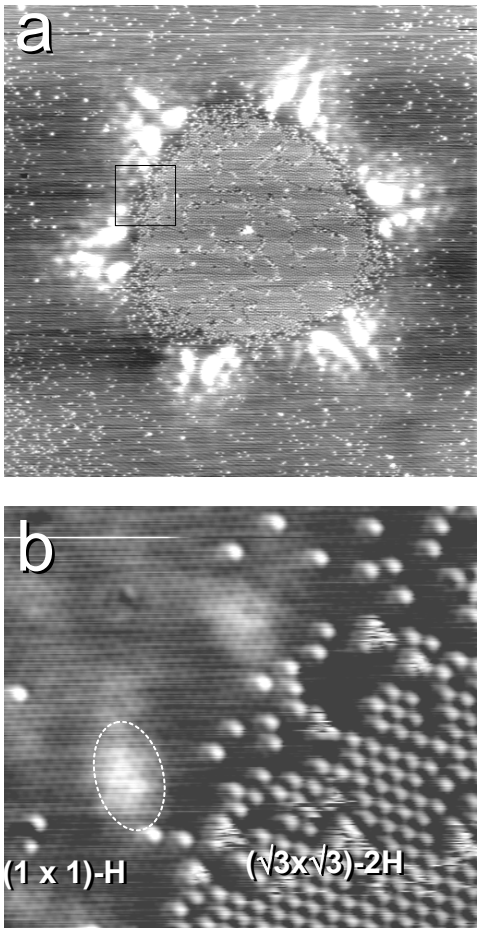

Figure 2. (a) 60x60 nm STM image of a H-covered Pd(111) surface (2nA, 200mV) 90 seconds after application of a 3 V pulse for 10 s between tip (located at the center) and surface. A region with rounded edges depleted of H has been created. The internal structure is $\sqrt{3}\times\sqrt{3}$ R30-2H (0.66 monolayers) with bright spots corresponding to H vacancies. (b) Expanded view (11x11 nm) of an area near the border (marked by a box in (a)). The region outside is covered by H in a 1x1 pattern. Brighter regions, like the one enclosed by an oval, are 60 to 100 pm higher that the surrounding. They are associated with a local coverage higher than 1, with the additional H in the second layer.

gave rise to brighter and larger triangles surrounded by dark regions (fig.1c-e). The size of the triangular region saturated at around 30 nm after a cumulative pulse length of 500 ms. Longer pulses (or a large number of short pulses in the same spot) resulted in the formation of additional bright satellite spots with 6-fold symmetry located outside the triangle, as shown in figs 1e after an accumulated 12.6 s pulse. The sides of the triangle are parallel to {1$\underline{1}$0}directions. The effect of electric field intensity was explored by increasing the voltage, and by decreasing the distance of the tip to the surface. The linear dimensions of the pattern increased with field strength, as shown in figure 1f, where the side of the triangle produced by a 10 s pulse is plotted versus voltage for two different tip-surface separations. From the ratio of gap resistances during tunneling conditions (12.5 Mohm / 100 Mohm) we calculated the tip-surface separation to decrease by about 0.2 nm from the bottom to the top graph. Longer duration pulses or higher voltages produce a more rounded shape of the H-depleted regions in addition to the bright satellite spots surrounding the triangle in a 6-fold symmetric pattern, as shown in fig. 1e. For voltages below 3 V, the results were independent of bias sign.

The atomic structure inside the triangles was √3x√3-1H, √3x√3-2H, or a mixture of both, as shown in fig. 2a. In the darker regions surrounding the triangle the structure is a nearly perfect 1x1, as shown in fig. 2b, which corresponds to the area in the box in fig. 2a. The

periodicity inside very bright regions decorating the triangles (like the one inside the dashed circle) is also 1x1 but is ~60 pm higher than the surrounding area. The increased height in these regions is attributed to the expansion of the Pd interlayer spacing due to H atoms below the surface, as discussed below.

The patterns generated by the voltage pulses can be explained as a result of redistribution of H induced by the electric field. The quasi-triangular symmetry of the H-depleted regions can be explained by the directionality of the diffusion events. In a previous paper, we have shown that H diffusion over bridge sites that are not adjacent to H-occupied sites is much more favorable than diffusion over top sites, which gave rise to triangular aggregates of vacancies with sides aligned in {1$\underline{1}$0} directions. The diffusion of H away from the central region under the tip generates a concentration gradient with spots of high H concentration that drives H to diffuse under the surface. As we will show the electric field affects the H adsorption energy. Since energy affects both equilibrium and kinetics in an exponential way, the electric field effects decrease also exponentially away from tip apex projection. For that reason, unless the tip is very flat, only the atomic structure near the apex is important, which explains the symmetric structure of the H concentration patterns. As the wave of H atoms diffusing away from the center abruptly slows

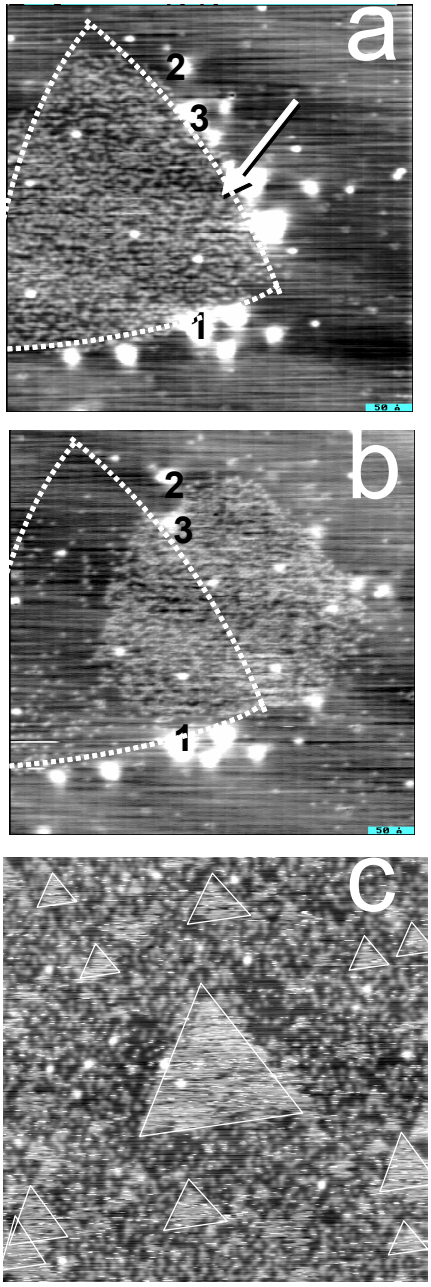

Figure 3. (a) 50x50 nm STM image (T = 86 K) showing a triangular region of depleted H after application of a 2 V pulse for 10 s. (b) Same region after a second pulse at the position marked by the arrow. Dashed lines mark the position of the initial triangle. The electric field redistributed H, "erasing" the original triangle and "writing" a new one. Bright protrusions are marked for reference. (c) Multiple H-depleted triangles produced by a 2 V pulse using a multiasperity tip.

down, it gives rise to spots of high concentration. It is in these high concentration spots, we think, that H diffuses into the bulk, producing the bright patches that surround the triangular H-depleted regions. The triangular features of reduced H density slowly decay over tens of minutes at 40-60 K as H diffuses back into the depleted zone. Interestingly, the triangular outline is still recognizable during most of this process, since the H diffusion inside the border than across the border due to the lower coverage.

An interesting characteristic of the H-patterns is that they are "erasable" by electric fields, as shown in Figure 3. Image (a) shows a roughly triangular region produced by a 2 V pulse. A second pulse was subsequently applied in the position marked by the arrow. As shown in image (b), a new triangular region is produced, effectively erasing the previous one. A few bright spots are numbered in the images for reference. The patterning capabilities of this method are illustrated in image (c) obtained with a multiasperity tip (such blunt tips are sometimes produced after mechanical contact with the sample). A triangular H-depleted region is produced at the projected position of each minitip.

To explain these observations, we performed self-consistent DFT calculations[20] using DACAPO[21], and determined the adsorption energy of atomic H (BE_H) as a function of coverage and electric field strength. The results of our calculations are shown in figure 4, where the average adsorption energy E_H of a H atom is plotted as a function of electric field strength for various coverages (θ_H). As can be seen, for each value of θ_H, the absolute value of BE_H is maximum at zero electric field and decreases with increasing field strength. As shown in the supplementary information, for H coverage less or equal to 1ML, this destabilization originates from the lack of dipole-moment differences and polarizability differences

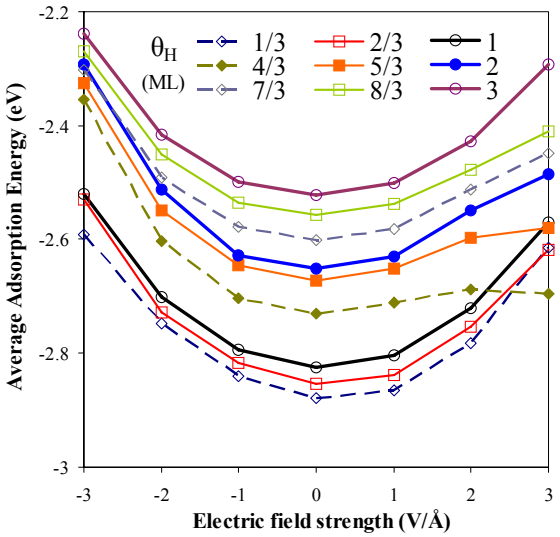

Figure 4. Calculated average adsorption energy of H on Pd(111) at various coverages from 1/3 ML to 3 ML, for a range of electric fields. Coverages above one correspond to H filling subsurface sites.

between the clean Pd and the H-covered Pd in combination with the polarizability of gas phase H. The latter accounts for the observed decrease in the average BE_H. In turn, this destabilization provides the thermodynamic driving force for the surface diffusion of H away from the tip, where the electric field is high, towards regions where the field is low. For coverages higher than 1ML, population of subsurface sites leads to a significant charge redistribution near the surface, with a concomitant significant increase in the field-induced dipole. This tends to stabilize adsorbed H, partially offsetting the polarizability-related destabilization effect (for more details see supplementary information). The complex interplay between field-induced dipole and polarizability effects, which vary with coverage and electric field strength, are responsible for the binding energy features shown in Fig. 4.

Fig. 4 also shows that, as θ_H increases E_H decreases, reflecting the repulsive interaction between coadsorbed H atoms. Interestingly, as mentioned above, at θ_H = 4/3 ML the presence of 1/3ML of H in the subsurface layer appears to stabilize the H atoms at higher positive electric fields. This further supports the model proposed above where the bright broad spots in the images near the periphery of the H-depleted islands correspond to regions of subsurface H. The electric field has therefore the dual effect of: (a) driving H away from the high field regions, thereby increasing the concentration in the periphery; and (b) stabilizing subsurface H states. Unfortunately the precise value of the electric field in the experiments can only be estimated, due to incomplete knowledge of the tip shape and tip-surface distance. Simple division of voltage (for 3 V) by tip-sample distance (~5 A) gives fields of about 0.6 V/A, clearly smaller than the largest electric fields probed theoretically and displayed in figure 4; yet, the theoretically predicted trends are quite robust.

There are two other important results from the DFT calculations. One is that the projected density of states at the Fermi level as function of coverage beyond 1 ML is essentially unchanged. The second is that there is an expansion of the Pd-Pd interlayer distance due to subsurface H atoms, resulting in an upward shift of the top Pd layer by 120 and 290 pm for the 4/3 ML and 2 ML respectively, relative to the full surface monolayer (1 ML) case. These results are in line with the contrast enhancement of the bright regions surrounding the triangles. The measured value of 60 pm is about half that

predicted by the calculations, which might correspond to a lower concentration of subsurface H in the experiments. H migration from surface to subsurface appears to be rather facile in Pd(111),as shown by our minimum energy path calculations[22] for diffusion of H on and in Pd(111), which yield activation energy barriers of 0.15eV and 0.40eV respectively.[23]

In conclusion, our results show that electric fields are an important parameter that can affect adsorbate concentration and mobility on the surface of metal catalysts, including electrocatalysts. With the advent of modern developments in nanofabrication of addressable metal nanoelectrodes near surfaces[24], one can envision the utilization of electric fields to generate specific patterns and reactivities on surfaces of interest.

Methods section:

A five-layer slab and a $\sqrt{3}\times\sqrt{3}$ surface unit cell were periodically repeated in a supercell geometry with five equivalent layers of vacuum between successive metal slabs. Adsorption was allowed on only one of the two surfaces exposed, and the electrostatic potential was adjusted accordingly[25]. The top three layers of the slab were allowed to relax. Ionic cores were described by ultrasoft pseudopotentials[26] and the Kohn-Sham one-electron valence states were expanded in a basis of plane waves with kinetic energy below 25 Ry. The surface Brillouin zone was sampled at 18 special Chadi-Cohen **k**-points[27]. The exchange-correlation energy and potential were described by the generalized gradient approximation (GGA-PW91)[28, 29]. The self-consistent PW91 density was determined by iterative diagonalization of the Kohn-Sham Hamiltonian, Fermi population of the Kohn-Sham states (k_BT=0.1eV) and Pulay mixing of the resulting electronic density[30]. Energies were extrapolated to k_BT = 0eV. The calculated bond energy for H_2(g) was 4.57eV, in reasonable agreement with the experimental value of 4.52eV at 298K[31]. Homogeneous external electric fields were imposed in our periodic calculations, as recently demonstrated by Rossmeisl et. al.[12] For each electric field, the total energies of: gas phase species, clean metal slab, and the slab with adsorbed species on/in it, were used to calculate the respective binding energies. For each specific electric field, BE_H is referred to a gas phase H atom and clean Pd(111) slab at infinite separation

from each other. The lattice constant of bulk Pd is calculated to be 0.399 nm, in good agreement with the experimental value of 0.389 nm[32].

References:

[1] C. N. Satterfield, *Heterogeneous Catalysis in Industrial Practice*, 2nd ed., Krieger Pulishing Company, Malabar, **1996**.
[2] J. Greeley, M. Mavrikakis, *Journal of Physical Chemistry B* **2005**, *109*, 3460.
[3] *Handbook of Fuel Cells: Fundamentals, Technology, Applications*, Wiley, West Sussex, **2003**.
[4] J. Greeley, J. K. Norskov, L. A. Kibler, A. M. El-Aziz, D. M. Kolb, *Chemphyschem* **2006**, *7*, 1032.
[5] S. Holloway, J. K. Norskov, *Journal of Electroanalytical Chemistry* **1984**, *161*, 193.
[6] P. S. Bagus, C. J. Nelin, W. Muller, M. R. Philpott, H. Seki, *Physical Review Letters* **1987**, *58*, 559.
[7] D. K. Lambert, *Journal of Chemical Physics* **1991**, *94*, 6237.
[8] M. Head-Gordon, J. C. Tully, *Chemical Physics* **1993**, *175*, 37.
[9] F. Illas, F. Mele, D. Curulla, A. Clotet, J. M. Ricart, *Electrochimica Acta* **1998**, *44*, 1213.
[10] M. T. M. Koper, R. A. van Santen, *Journal of Electroanalytical Chemistry* **1999**, *472*, 126.
[11] S. A. Wasileski, M. T. M. Koper, M. J. Weaver, *Journal of the American Chemical Society* **2002**, *124*, 2796.
[12] J. Rossmeisl, J. K. Norskov, C. D. Taylor, M. J. Janik, M. Neurock, *Journal of Physical Chemistry B* **2006**, *110*, 21833.
[13] E. C. H. Sykes, L. C. Fernandez-Torres, S. U. Nanayakkara, B. A. Mantooth, R. M. Nevin, P. S. Weiss, *Proceedings of the National Academy of Sciences of the United States of America* **2005**, *102*, 17907.
[14] T. C. Shen, C. Wang, G. C. Abeln, J. R. Tucker, J. W. Lyding, P. Avouris, R. E. Walkup, *Science* **1995**, *268*, 1590.
[15] G. L. Kellogg, T. T. Tsong, P. Cowan, *Surface Science* **1978**, *70*, 485.
[16] S. Behler, M. K. Rose, J. C. Dunphy, D. F. Ogletree, M. Salmeron, C. Chapelier, *Review of Scientific Instruments* **1997**, *68*, 2479.
[17] T. Mitsui, M. K. Rose, E. Fomin, D. F. Ogletree, M. Salmeron, *Surface Science* **2003**, *540*, 5.
[18] T. Mitsui, M. K. Rose, E. Fomin, D. F. Ogletree, M. Salmeron, *Nature* **2003**, *422*, 705.
[19] N. Lopez, Z. Lodziana, F. Illas, M. Salmeron, *Physical Review Letters* **2004**, *93*.
[20] J. Greeley, J. K. Nørskov, M. Mavrikakis, *Annual Review of Physical Chemistry* **2002**, *53*, 319.
[21] B. Hammer, L. B. Hansen, J. K. Nørskov, *Phys. Rev. B* **1999**, *59*, 7413.
[22] G. Henkelman, H. Jónsson, *Journal of Chemical Physics* **2000**, *113*, 9978.

[23] Minimum energy paths for diffusion were uniformly upshifted in energy in the presence of non-zero electric fields, but the corresponding diffusion barriers remain practically invariant in the existence of such fields.
[24] X. M. Yan, S. Kwon, A. M. Contreras, J. Bokor, G. A. Somorjai, *Nano Letters* **2005**, *5*, 745.
[25] J. Neugebauer, M. Scheffler, *Phys. Rev. B* **1992**, *46*, 16067.
[26] D. Vanderbilt, *Physical Review B* **1990**, *41*, 7892.
[27] D. J. Chadi, M. L. Cohen, *Physical Review B* **1973**, *8*, 5747.
[28] J. P. Perdew, J. A. Chevary, S. H. Vosko, K. A. Jackson, M. R. Pederson, D. J. Singh, C. Fiolhais, *Phys. Rev. B* **1992**, *46*, 6671.
[29] J. A. White, D. M. Bird, *Phys. Rev. B* **1994**, *50*, 4954.
[30] G. Kresse, J. Furthmuller, *Comput. Mater. Sci.* **1996**, *6*, 15.
[31] D. R. Lide, *CRC Handbook of Chemistry and Physics*, 76 ed., CRC Press: New York, **1996**.
[32] N. W. Ashcroft, N. D. Mermin, *Solid State Physics, Vol. 1*, Saunders College, Orlando, FL, **1976**.